Predicting Phase Synchronization for Homoclinic Chaos in a CO_2 Laser

Isao Tokuda*, Jürgen Kurths*, Enrico Allaria†, Riccardo Meucci**, Stefano Boccaletti** and F. Tito Arecchi†

* *Nonlinear Dynamics, Institute of Physics, University of Potsdam, D-14415, Potsdam, Germany*
† *Department of Physics, University of Florence, 50019, Firenze, Italy*
** *Istituto Nazionale di Ottica Applicata, Largo E. Fermi, 6 I50125 Firence, Italy*

Abstract. A novel approach is presented for the reconstruction of phase synchronization phenomena in a chaotic CO_2 laser from experimental data. We analyze this laser system in a regime of homoclinic chaos, which is able to phase synchronize with a weak sinusoidal forcing. Our technique recovers the synchronization diagram of the experimental system from only few measurement data sets, thus allowing the prediction of the regime of phase synchronization as well as non-synchronization in a broad parameter space of forcing frequency and amplitude without further experiments.

INTRODUCTION

Synchronization is a fundamental phenomenon of coupled or forced nonlinear oscillators, which is nowadays attracting a significant interest of natural science and engineering. Up to date four basic types of synchronization, namely, complete [1, 2], generalized [3], phase [4], and lag synchronization [5], have been found. Phase synchronization (PS) of coupled or periodically forced complex systems has found many applications both in laboratory experiments and in natural systems [6, 7].

To analyze data from such experimental systems, special techniques for PS analysis have been developed and it has been shown that they are very efficient even for noisy and non-stationary data [7, 8]. However, the problem of reconstructing models from such synchronized data remains open. By using such models, it is of special interest to infer a synchronization diagram which yields the regimes of PS, non-PS, and borderlines between both, which are dependent upon the system parameters, such as the coupling strength and the forcing frequency of interacting nonlinear oscillators. By recovering such synchronization diagram from few sets of experimental data, a deeper insight into the underlying system can be gained. This problem formulation is quite practical in situations, where an extensive synchronization experiment is not possible or very expensive and only limited sets are recorded. To retrieve the synchronization regime, reconstruction of a family of models, which is parameterized by the coupling strength and the forcing frequency, from recording data is required. In a recent study, we have introduced a novel technique for constructing such a parameterized family of coupled nonlinear models based on an artificial neural network and its parameter reduction by singular value decomposition [9]. Our technique has been successfully applied to

CP742, *Experimental Chaos: 8th Experimental Chaos Conference,* edited by S. Boccaletti et al.
© 2004 American Institute of Physics 0-7354-0226-4/04/$22.00

Downloaded 31 Oct 2005 to 150.65.7.70. Redistribution subject to AIP license or copyright, see http://proceedings.aip.org/proceedings/cpcr.jsp

prototypical PS models and to experimental data from a paced plasma discharge tube, where all of the dynamics were rather phase-coherent. However, the technique is not straightforwardly applicable to more complex systems such as fast-slow dynamical systems, which are quite common in nature and engineering.

This paper extends this approach [9] to the case of a homoclinic chaos and apply it to experimental data from a CO_2 laser [10]. This laser has been known as one of the earliest systems that verified the existence of Shil'nikov-type chaos [11] in real experiments. Under certain conditions, the output intensity of the laser consists of a series of homoclinic spikes with chaotic time intervals [10]. Due to its similarities to electrochemical spike trains traveling on the axons of biological neurons, the laser is considered as an prototypical experimental system for the study of neural activity. With a weak sinusoidal forcing, the homoclinic chaos is able to phase synchronize, where the regime of PS gives rise to a clear Arnold tongue structure [12]. By the extended approach, we demonstrate that the synchronous behavior of the laser system is modeled from only three sets of data, obtained from measurements made with different forcing conditions.

EXPERIMENTAL SYSTEM

Fig. 1 (a) shows a single mode CO_2 laser with feedback. The optical cavity, 1.35 m long, is defined by a reflecting grating (M1) acting as a totally reflecting mirror at the desired wavelength (10.6 μm) and a partially reflecting mirror (M2). The laser medium, a gas mixture of CO_2, He, H, and N_2, is excited by a discharge current of 6 mA applied to the laser tube closed by two Brewster windows. The laser cavity also contains an electro-optic modulator which controls the cavity losses by a feedback signal proportional to the laser output intensity. By acting on the two control parameters of the feedback loop, the gain and the bias voltage (B_0), we can set the system in a condition where the output intensity consists of a train of homoclinic spikes [10]. Fig. 1 (b) shows such homoclinic spikes repeating with chaotic time intervals, where the averaged spiking frequency is approximately 1.435 kHz (a time interval between one spike to the next is regarded as one period in our PS analysis). It has been clarified that the homoclinic spikes are generated by the Shil'nikov-type mechanism [11] associated with a saddle focus point located near the origin. The typical characteristic of the laser is its fast-slow dynamical structure. Namely, the laser dynamics is quite slow near the saddle point, whereas it is much faster outside the homoclinicity.

By applying an external perturbation to the electric discharge, the chaotic laser system can synchronize with a sinusoidal perturbation $y(t) = I\, sin(2\pi\nu t)$ [12]. By means of a PC board (NI PCI-6040E) and an acquisition routine on LabView, we constructed the synchronization diagram by varying the forcing parameters as $(\nu, I) \in$ [1 kHz: 2kHz] $\times$ [0% : 3%] (Fig. 2, right). Then, for testing and validating our method, the laser intensity $x(t)$ and the external modulation $y(t)$ were simultaneously measured. The recording was made for 3 different parameter sets $(\nu, I) = (0[\text{kHz}], 0[\%])$, $(1.1[\text{kHz}], 1.5[\%])$, $(1.7[\text{kHz}], 1.5[\%])$, which are all in a regime of non-PS. Based on only the three sets of the bivariate data $\{x(t), y(t)\}$, our task is to predict for which parameters of forcing

Downloaded 31 Oct 2005 to 150.65.7.70. Redistribution subject to AIP license or copyright, see http://proceedings.aip.org/proceedings/cpcr.jsp

frequency ν and amplitude I the forced system is in the regime of PS.

This condition is practical for experimental situations, where an extensive exploration of the synchronization phenomena is not possible. For instance, in neuroscience, a response characteristic of a single neuron to sinusoidal forcing provides an important clue. Due to its limited life-time, however, it is almost impossible to investigate the response property of the physiological neuron to every combination of the forcing frequency and the amplitude. It is therefore a strong challenge to estimate the synchronization diagram from only a few sets of recording data.

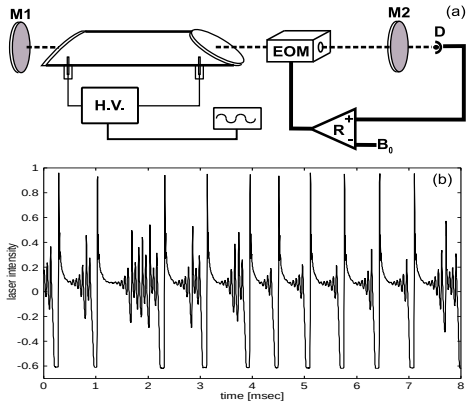

FIGURE 1. Experimental setup of the CO_2 laser with feedback (upper) and time series $\{x(t)\}$ of the laser intensity recorded without forcing (lower).

MODELING TECHNIQUE

Main points of our modeling technique for the forced homoclinic system are as follows. First, we embed the bivariate time series $\{x(t), y(t)\}$ into delay coordinates $X(t) = \{x(t), x(t-\tau), \ldots, x(t-(d-1)\tau)\}$, $Y(t) = \{y(t), y(t-\tau), \ldots, y(t-(d-1)\tau)\}$ (d: embedding dimension, τ: time lag) and suppose according to the embedding theorem [13] that there exists the following dynamics

$$x(t+1) \quad = \quad F(X(t), Y(t)). \tag{1}$$

Second, we construct a nonlinear function $\tilde{F}$, that approximates Eq. (1). Since the function F is in an input-output form, which requires rather complex modeling, we make a simplification. Namely, according to the property of PS, which is induced by only a small forcing strength, we assume that the intensity of the forcing is much smaller than that of the forced system ($|y| \ll |x|$) and via a first order approximation we obtain:

$$x(t+1) = F(X(t)) + \alpha_1 I \sin(2\pi\nu t) + \alpha_2 I \cos(2\pi\nu t) \tag{2}$$

Then we model the forced homoclinic chaos with an approximate nonlinear function $\tilde{F}$. If the original forced dynamics is precisely modeled, the regime of PS as well as

Downloaded 31 Oct 2005 to 150.65.7.70. Redistribution subject to AIP license or copyright, see http://proceedings.aip.org/proceedings/cpcr.jsp

non-PS in the parameter space of forcing frequency ν and amplitude I can be predicted by studying the model $\tilde{F}$. A practical modeling procedure is to optimize all parameters $\{\Omega, \alpha\}$ of the model function $\tilde{F}$ by minimizing the cost function:

$$E_D(\Omega, \alpha) = \sum_{t,I,\nu} \{x(t+1) - \tilde{F}(\Omega, X(t)) - \alpha_1 I \sin(2\pi\nu t) - \alpha_2 I \cos(2\pi\nu t)\}^2. \quad (3)$$

The modeling of the homoclinic system requires a careful treatment because of its fast-slow dynamical property. To recover the global dynamics, a simultaneous modeling of both slow and fast dynamics is indispensable. Since the homoclinicity determines the global dynamical property, it is in particular important to precisely model the local structure near the homoclinicity. To deal with this problem, the radial basis function (RBF) [14, 15]

$$\tilde{F}(\Omega, X) = \sum_k \Omega_k \, \phi(\sigma_k, \|X - c_k\|) \quad (4)$$

is exploited, where ϕ and c_k stand for the basis function and the centroid and $\|\cdot\|$ denotes the Euclidean norm. Although the RBF is a global functional approach, it has a local property, which is suitable for the modeling of the delicate dynamics near the homoclinicity [15].

Our modeling procedure consists of the following main steps:

(P1) The embedding dimension d and the time lag τ are chosen. The time lag is chosen so that the structure of the two-dimensional unstable manifold of the saddle focus point is fully unfolded. This is crucial for a precise modeling of the homoclinic structure. The embedding dimension is set to be three, since a low-dimensional model is preferred for simplicity and dimension three is in general sufficient to model the homoclinicity [11].

(P2) Due to the fast-slow dynamics, equally sampled data concentrate much more densely near the homoclinicity than outside. For modeling both the fast and slow dynamics with a good balance, we scatter the data points. First, we define the slow data as $\{X(t) : |x(t+1) - x(t-1)|/(2.0 \cdot \Delta t) < \Theta_v\}$, where the threshold Θ_v is chosen so that the points near the homoclinicity are separated from the others. All other data are regarded as fast data. Then among the slow data set, a subset of data satisfying $\{\|X(t) - X(s)\| > \Theta_s, \ \forall\, t, s\}$ is extracted. In the same way, a subset of the fast data satisfying $\{\|X(t) - X(s)\| > \Theta_f, \ \forall\, t, s\}$ is extracted.

(P3) From both of the fast and the slow data, the same number of centroids $\{c_k\}$ is randomly selected with an addition of noise. The centroids with additive noise, called *chaperons*, have been successfully applied to the modeling of homoclinic dynamics from string data [15].

(P4) As a basis function, Gaussian RBF, $\phi(\sigma_k, r) = \exp(-r^2 \,/\, \sigma_k^2)$, with an inhomogeneous variance parameter, $\sigma_k^2 = \min_{i \neq k} \|\mathbf{c}_i - \mathbf{c}_k\|^2$, is used. Due to the fast-slow property, centroids selected in (P3) are located not uniformly in the data space. The inhomogeneous parameters are effective for interpolating such nonuniform centroids.

(P5) The model parameters $\{\Omega, \alpha\}$ are optimized by the least-square-error algorithm of the cost function $E = E_D + \beta\{\sum_k \Omega_k^2 + \sum_k \alpha_k^2\}$, where the first term corresponds to the fitting error of Eq. (3) and the second term corresponds to the regularizer. The regularizing constant β is chosen in such a way that a natural frequency of the nonlinear model is close to the one of the original system.

Downloaded 31 Oct 2005 to 150.65.7.70. Redistribution subject to AIP license or copyright, see http://proceedings.aip.org/proceedings/cpcr.jsp

(P6) By changing the frequency ν and the amplitude I of the forced model, $x(t+1) = \tilde{F}(X(t)) + \alpha_1 I \sin(2\pi\nu t) + \alpha_2 I \cos(2\pi\nu t)$, the model frequency $\tilde{\nu}$ is computed by its free-running. The synchronization diagram is finally drawn with a relative frequency difference between the model and the forcing as $\Delta\nu = (\tilde{\nu} - \nu) / \nu$.

RESULTS

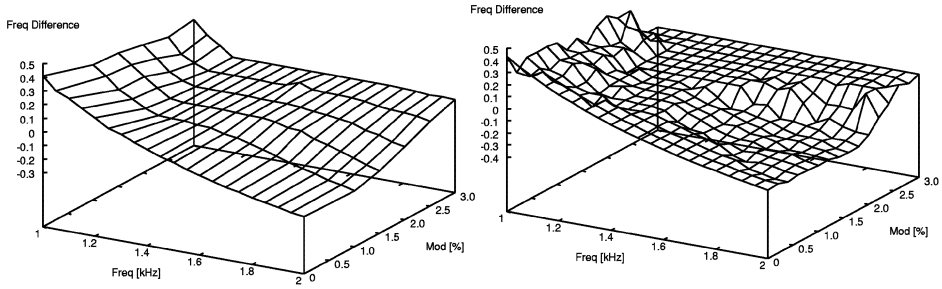

FIGURE 2. Relative frequency difference $\Delta\nu$ of the laser experiment (left) and the model (right), depending upon the forcing frequency and amplitude, which are varied as $(\nu, I) \in$ [1 kHz: 2kHz] $\times$ [0% : 3%].

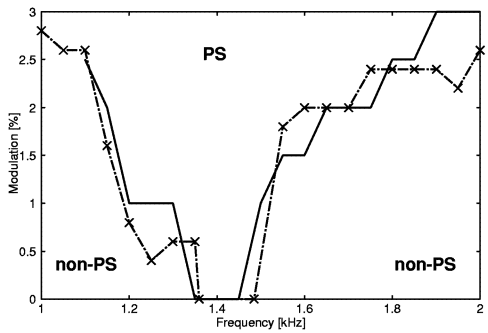

FIGURE 3. Borderlines between regimes of PS and non-PS for the laser (solid line) and the model (dotted line with crosses).

To apply our modeling to the laser experiment, the embedding dimension, the time lag, and the thresholds were set as $(d, \tau, \Theta_v, \Theta_s, \Theta_f) = (3, 10[\mu s], 0.0075, 0.012, 0.016)$. From each of the fast and the slow data from a non-forcing experiment, 300 chaperons were randomly selected with an addition of 30% noise of the data. By varying the regularizing parameter in $\beta \in$ [0.9: 1.1], we have confirmed that the nonlinear model yields a natural frequency of $\tilde{\nu} = 1.435$ at $\beta = 1.05$, which coincides in a good accuracy with the laser's original frequency measured from the non-forcing experiment. We therefore exploited the nonlinear model optimized with the regularizing parameter $\beta = 1.05$. Fig. 2 gives synchronization diagram of the original laser (left) and the nonlinear model (right). The model diagram shows a strong similarity to the original.

Downloaded 31 Oct 2005 to 150.65.7.70. Redistribution subject to AIP license or copyright, see http://proceedings.aip.org/proceedings/cpcr.jsp

Fig. 3 shows borderlines between the regimes of PS and non-PS were for the original laser and the nonlinear model, where the regime of PS was defined as $|\Delta\nu| < 0.05$ [12]. Again the model diagram is in a very good agreement with the experimental.

CONCLUSIONS

To conclude, the modeling approach enables the reconstruction of a synchronization diagram of a forced homoclinic system from only a few experimental records of bivariate time series. The difficulty of modeling the global dynamical property of the homoclinic chaos has been overcome by using the RBF, which is relatively simple to implement. With an application to the experimental data of the CO_2 laser, our technique was capable of predicting the regime of PS as well as non-PS in the parameter space of forcing frequency and amplitude without further experiments. This approach should be of significant importance especially for neuroscientific data, where extensive synchronization analysis in a single neuron is quite difficult due to its short life-time and reproduction of the same experiment with another neuron is almost impossible. Another important future study is to extend our approach to a network of coupled oscillators, which has many applications to synchronization of spatio-temporal systems such as electrochemical oscillators [16] or brain activity [8].

REFERENCES

1. H. Fujisaka and T. Yamada, Prog. Theor. Phys., **69**, 32 (1983).
2. L.M. Pecora and T.L. Carroll, Phys. Rev. Lett. **80**, 2109 (1990).
3. N.F. Rulkov, M.M. Sushchik, L.S. Tsimring, and H.D.I. Abarbanel, Phys. Rev. E **51**, 980 (1995); L. Kocarev and U. Parlitz, Phys. Rev. Lett. **76**, 1816 (1996); K. Josic, Phys. Rev. Lett. **80**, 3053 (1998).
4. M.G. Rosenblum, A.S. Pikovsky, and J. Kurths, Phys. Rev. Lett. **76**, 1804 (1996).
5. M.G. Rosenblum, A.S. Pikovsky, and J. Kurths, Phys. Rev. Lett. **78**, 4193 (1997).
6. J. Kurths (Ed.), *Phase Synchronization and its Applications*, Special Issue in Int. J. Bifurcation and Chaos, **10-11** (2000).
7. A. Pikovsky, M. Rosenblum, and J. Kurths *Synchronization - A Universal Concept in Nonlinear Sciences*, (Cambridge University Press, Cambridge, 2001).
8. P. Tass *et al.*, Phys. Rev. Lett. **81**, 3291 (1998).
9. I. Tokuda, J. Kurths, E. Rosa Jr., Phys. Rev. Lett. **88**, 014101 (2002).
10. F.T. Arecchi, R. Meucci, and W. Gadomski, Phys. Rev. Lett. **58**, 2205 (1987).
11. L.P. Shil'nikov, Sov. Math. Dokl. **6**, 163 (1965).
12. E. Allaria, F.T.Arecchi, A. DiGarbo, and R. Meucci, Phys. Rev. Lett. **86**, 791 (2001).
13. F. Takens, in *Dynamical Systems and Turbulence*, Lecture Notes in Math., edited by D. A. Range and L.S. Young (Springer, Berlin, 1981), Vol. 898, p. 366; T. Sauer, J.A. York, and M. Casdagli, J. Stat. Phys. **65**, 579 (1991).
14. M. Casdagli, Physica **35D**, 335 (1989).
15. K. Judd and A.I. Mees, Physica D **82**, 426 (1995); Physica D **92**, 221 (1996).
16. W. Wang, I.Z. Kiss, and J.L. Hudson, Phys. Rev. Lett. **86**, 4954 (2001).

Downloaded 31 Oct 2005 to 150.65.7.70. Redistribution subject to AIP license or copyright, see http://proceedings.aip.org/proceedings/cpcr.jsp